8-2019

Comparing the Efficacy of Pharmacological Preconditioning with Myristic Acid-conjugated, TAT- conjugated and Native Protein Kinase C Epsilon Peptide Activator in Myocardial Ischemia/ Reperfusion (MI/R) Models

Anahi McIntyre
Philadelphia College of Osteopathic Medicine

Philadelphia College of Osteopathic Medicine

School of Health Sciences

Graduate Program in Biomedical Sciences

Comparing the Efficacy of Pharmacological Preconditioning with Myristic Acid-conjugated, TAT- conjugated and Native Protein Kinase C Epsilon Peptide Activator in Myocardial Ischemia/Reperfusion (MI/R) Models

A Thesis in Biomedical Sciences by Anahi McIntyre

Submitted in Partial Fulfillment of the Requirements for the Degree of

Master of Science in Biomedical Sciences

August 2019

We, the undersigned, duly appointed committee have read and examined this manuscript and certify it is adequate in scope and quality as a thesis for this master's degree. We approve the content of the thesis to be submitted for processing and acceptance.

_____ _____

Lindon Young Ph.D., Thesis Advisor
Professor of Pharmacology
Department of Bio-Medical Sciences

Date

_____ _____

Robert Barsotti, Ph.D., Thesis Committee Member
Professor of Physiology
Department of Bio-Medical Sciences

Date

_____ _____

Cathy Hatcher, Ph.D., Thesis Committee Member
Associate Professor of Physiology
Department of Bio-Medical Sciences

Date

ABSTRACT

Protein kinase C epsilon (PKCε) activation is a central mediator of the cardioprotection conferred by myocardial ischemic preconditioning (IPC). PKCε activation via PKCε peptide activator (PKCε+, HDAPIGYD) prior to ischemia is a pharmacologic mimic of IPC. However, native PKCε+ requires the use of cell permeabilization methods, such as conjugation to known carrier peptides, for effective intracellular targeting to mitigate cardiac damage. Our study compares PKCε+ conjugated to either myristic acid (Myr-PKCε+) or transactivating (TAT) carrier peptide (YGRKKRRQRRR-CC- PKCε+) with native PKCε+ pretreatment and untreated control I/R hearts to evaluate the efficacy of these cell permeable peptide analogs in attenuating contractile dysfunction and infarct size after MI (30min)/R (90min). Infarct size was assessed by 1% triphenyltetrazolium chloride staining of heart tissue, which was evaluated using NIH ImageJ software pixel analysis and weight dissection analysis. ImageJ pixel analysis showed significantly reduced infarct size in the Myr-PKCε+ (29±1%, $p<0.05$) and TAT-PKCε+ (25±2%, $p<0.01$) pretreated hearts compared to native PKCε+ pretreated (34±2%) and control I/R hearts (35±2%). By contrast, only TAT-PKCε+ pretreated hearts (26±2%, $p<0.01$) exhibited significant difference from native PKCε+ pretreated hearts (35±2%) and control hearts (36±2%) when evaluated via weight dissection. Despite significant improvement in infarct size, there was no significant improvement in post-perfused cardiac function across all groups. These results indicate that PKCε+ conjugation to either Myr or TAT significantly improved its efficaciousness in attenuating infarct size when given before ischemia. Further, this improvement was independent of cardiac

function. These results suggest that Myr- or TAT-conjugated PKCε+ may be an effective treatment to attenuate cell death in coronary bypass or organ transplantation settings.

TABLE OF CONTENTS

LIST OF FIGURES

LIST OF TABLES

INTRODUCTION

1.1 Background

1.1.1 Preconditioning and protein kinase C

Cardiovascular disease (CVD) is the leading cause of morbidity and mortality for adults in developed countries. Among these diseases myocardial infarction remains a major contributor to the healthcare burden of CVD [1]. This damage is initiated by complete or partial blockage of a coronary artery resulting in ischemia, a decrease in blood flow. Although timely reperfusion, or restoration, of blood flow into the ischemic myocardium is necessary for survival, the rapid restoration of physiological pH and generation of reactive oxygen species (ROS) by dysfunctional mitochondria and uncoupled endothelial nitric oxide synthase (eNOS) results in ischemic injury [2]. Attempts to reduce ischemic injury, characterized by irreversible cardiomyocyte damage and compromised heart function, have provided insight into several cardioprotective molecular mechanisms.

The cardioprotective effects of myocardial ischemic preconditioning (IPC), or brief nonlethal intervals of ischemia followed by intermittent reperfusion, prior to prolonged ischemia have been well established. IPC was first identified in 1986 by Murry et al. as an exogenous method to delay cell death and reduce infarct size [3]. Myocardial IPC is characterized by several cycles of brief ischemia (i.e. less than 4 min x3) followed by intermittent periods of reperfusion (i.e. less than 6 min x3) prior to prolonged ischemia (i.e. greater than 30 min) [4]. This is an adaptive response to protect the heart from the deleterious effects of prolonged ischemia during the final reperfusion phase.

Although initially poorly understood, over 20 years of research has identified diacyl glycerol (DAG) or ROS mediated activation of protein kinase C epsilon (PKCε) as a key effector involved in preconditioning (Figure 1) [5]. PKCε is an important enzymatic isoform of protein kinase C (PKC) with paradoxical roles before and after prolonged ischemia. While PKCε inhibition is cardioprotective only at the time of reperfusion, PKCε activation is cardioprotective prior to prolonged ischemic insult and serves as a means to mimic preconditioning [6, 7]. PKCε is necessary and sufficient to increase cellular resistance to ischemic injury [8, 9]. The observation that PKCε$^{-/-}$ knockout mice do not benefit from IPC while cardiac-specific PKCε overexpression confers cardioprotection similar to that of IPC have confirmed the central role of PKCε in preconditioning [8, 9].

The PKC family consists of several isoforms of Ser/Thr kinases with varying expression and differential activation. All PKC isoforms are activated in a G protein-mediated ($G\alpha_q$) signaling cascade resulting in the hydrolysis of phosphatidylinositol 4,5-bisphosphate (PIP_2) and inositol trisphosphate (IP_3) to produce DAG and release Ca^{2+} from the endoplasmic reticulum, respectively (Figure 1) [10]. While conventional PKC isoforms (cPKCs; α, βI, βII, and γ) require Ca^{2+} and DAG for activation, novel PKC isoforms (nPKCs; ε, δ, θ, and η) are activated by DAG independently of Ca^{2+}. Further, PKC atypical isoforms (nPKCs; λ/ι and ζ) are activated by sphingomyelins (lipid rafts) and are DAG and Ca^{2+} independent [10]. All PKC isoforms are variably expressed in many tissue of the body. In particular, PKCε is constitutively expressed in the heart, cerebellum, pancreas, ovaries, lungs, spleen, and adrenal glands (rats) [11]. Moreover, PKCε is highly expressed in human cardiac muscle and therefore suggests understanding this mechanism would be of high value clinically in heart attack and organ transplant patients [12].

Within cardiomyocytes, inactive PKCε is found in the cytosol and mitochondrial inner membrane [13]. While PKCε plays a role during cardiomyocyte differentiation and development, its targets within the adult rat heart are the focus of this study [14]. There are more than 36 known targets of PKCε. Of these PKCε activation of eNOS and cardiac mitochondria are putative targets for cardioprotection [13]. Regarding the mitochondria, basal levels of mitochondrial PKCε (mPKCε) located in the inner mitochondrial membrane are augmented by cytosolic PKCε which translocates to the mitochondria following activation [13, 15]. PKCε import into the mitochondria is mediated by heat shock protein 90 (HSP90) and proceeds via a mitochondrial import receptor, translocase of the outer membrane (Tom20) [16]. Whether already located in the mitochondria or imported in, PKCε phosphorylates mitochondrial K_{ATP} channels (mitoK_{ATP}) which results in opening of mitoK_{ATP}. This mechanism is helpful for ATP preservation and inhibition of mitochondrial permeability transition pore (MPTP) formation to prevent rupturing of the mitochondria [17]. While PKCε also translocates to cardiac sarcomeres acting as a key mediator in maladaptive hypertrophy, sarcomeric K_{ATP} (sarcoK_{ATP}) channel opening is not related to the cardioprotective mechanism of PKCε in I/R injury [18, 19].

1.1.2 Sources of oxidative damage during I/R central to the preconditioning mechanism

The finding that diazoxide, an mitoK_{ATP} channel agonist, acts as a IPC mimetic while 5-hydroxydecanoate (5-HD), an mitoK_{ATP} channel antagonist, eliminates preconditioning led to the hypothesis that mitoK_{ATP} channels were involved in preconditioning [20]. A link between PKCε and mitoK_{ATP} channels was confirmed when it was found that PKCε activation augments and accelerates channel opening [21]. Further, the cardioprotective effects of mitoK_{ATP} channel opening are blocked in the absence of PKCε indicating that mitoK_{ATP} channels may be

downstream of PKCε [20]. However, the ROS released by opened mitoK$_{ATP}$ channels directly activate PKCε through oxidation of its regulatory domain creating a positive feedback loop of activation and channel opening [22].

A second part of the mitochondrial preconditioning signal transduction system is the MPTP. This nonspecific pore spanning the inner and outer mitochondrial membranes opens during reperfusion leading to mitochondrial swelling, uncoupling of oxidative phosphorylation, and cytochrome c release. Unchecked mitochondrial permeability transition results in the collapse of mitochondrial membrane potential and cell death [23]. PKCε has been found to directly and indirectly inhibit MPTP opening via phosphorylation of key pore components and mitoK$_{ATP}$ channel opening, respectively [24, 25]. Prevention of pore inhibition significantly attenuates the cardioprotective effects of PKCε, indicating that the MPTP plays at least a partial role in the mechanism of PKCε mediated preconditioning [25].

Although the full mechanisms by which mitoK$_{ATP}$ channels and the MPTP are involved in preconditioning have yet to be elucidated, PKCε appears to be an essential effector. Costa and Garlid proposed a unique mechanism of PKCε induced cardioprotection effectively linking mitochondrial inner membrane associated PKCε with both mitoK$_{ATP}$ channels and the MPTP. Once the cardioprotective signaling pathway begins, activated cGMP-dependent protein kinase (PKG) transmits the signal to the mitochondria via phosphorylation of an unknown mitochondrial outer membrane protein (MOM). This signal is presumably transmitted to a first pool of mitochondrial PKCε (mPKCε1) in the mitochondrial inner membrane resulting in mitoK$_{ATP}$ opening which in turn stimulates ROS release from complex I of the respiratory chain.

The increase in ROS then activates a second pool of PKCε (mPKCε2) via oxidative modification of its regulatory domain which then phosphorylates and inhibits the MPTP (Figure 1) [17].

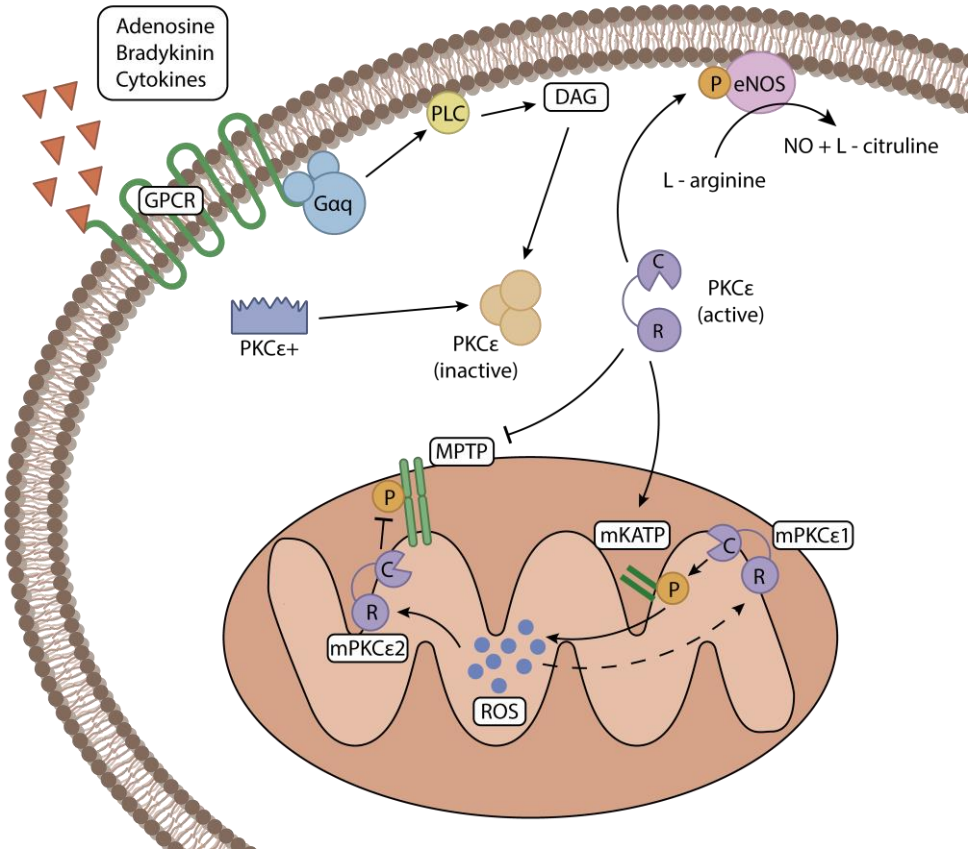

Figure 1. Schematic representation of PKCε activation and end effectors.
PKCε activation via DAG. ROS from dysfunctional mitochondria, and PKCε+ peptide activator. Activated PKCε then phosphorylates mitochondrial K_{ATP} channels (mK_{ATP}) and mitochondrial transition permeability pore (MPTP). Adapted from [17].

In addition to mitochondrial derived ROS, uncoupled eNOS is one of the major sources of damaging ROS during reperfusion [26]. PKCε is known to increase eNOS activity via phosphorylation at ser1177 [27]. Regarding cardiac activation of endothelial derived NO release in cardiac tissue, it has been shown that reducing NO release will decrease the coupling efficiency of mitochondrial O_2 consumption and ATP production, whereas increasing NO release

improves the coupling efficiency of the electron transport chain to produce the same amount of ATP with less O_2 consumption [28]. Therefore there would be less mitochondrial derived ROS produced from complexes I and III under conditions of NO synthesis which would occur prior to prolonged ischemia where eNOS is in its coupled state. However, this mechanism may not be helpful during reperfusion when the oxidation of eNOS cofactor tetrahydrobiopterin (BH_4) leads to dihydrobiopterin (BH_2) production which competes with BH_4 with equal affinity at the oxygenase domain of eNOS. Under these conditions eNOS cannot produce NO and instead produces superoxide which contributes to oxidative stress during reperfusion injury and increases in hydrogen peroxide (H_2O_2) in tissues [28, 29].

1.1.3 PKCε activator peptide

A pharmacological method by which to activate PKCε is an isoform-specific PKCε activator peptide (PKCε+), also known as ψεRACK peptide (Figure 1). PKC function is known to be mediated by anchoring proteins known as receptors for activated C kinase (RACK). Each PKC isozyme has a RACK-selective recognition site distinct from its substrate binding site. Activated PKC binds with high affinity to RACK, which translocates PKC to phosphorylate substrates at specific intracellular sites to produce a physiologic response [30, 31, 32]. This study utilizes several modifications of a well-established PKCε+ peptide (HDAPIGYD), also known as pseudo-εRACK (ψεRACK), as a chemical modality to mimic IPC [31]. Western blots and immunofluorescence have confirmed PKCε+-induced selective translocation of PKCε from cytosolic to particulate subcellular fractions which indicates PKCε activation. In $PKC\varepsilon^{+/+}$ overexpressed transgenic mice, PKCε+ improved cardiac function and reduced levels of creatine phosphokinase (CPK), a marker of cardiac damage in I/R hearts [33].

Although the mechanism of action of PKCε+ has yet to be elucidated, the predominant theory states that PKCε+ binds to inactive PKCε rendering it active, or in an "open" conformation that facilitates εRACK binding [10]. This occurs via PKCε+ binding to the εRACK binding site on PKCε, effectively disrupting the auto-inhibitory intramolecular interaction between its RACK-binding site and pseudo-RACK (ψεRACK) binding site. This interaction is due to PKCε+ homology to amino acids 85-92 (HDAPIGYD) on the V1 domain of PKCε. The transient conformational opening induced by PKCε+ is then stabilized by PKCε-εRACK binding (Figure 2). This switch may be due to the partial homology between PKCε+ and εRACK amino acids 285–292 (NNVALGYD) [32]. Once εRACK is bound to PKCε, PKCε is anchored in position to phosphorylate its intracellular targets.

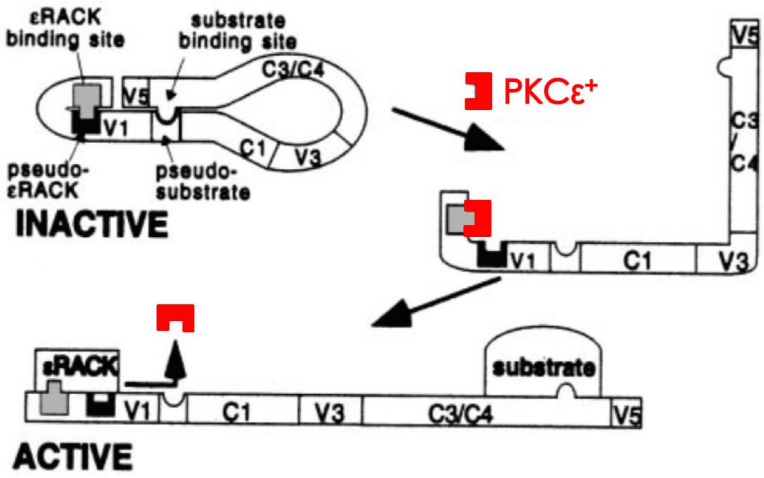

Figure 2. PKCε+ activates PKCε to facilitate RACK binding.

Proposed mechanism for PKCε activation by PKCε+ in which PKCε+ binds to the εRACK binding site to activate PKCε. εRACK then binds to stabilize PKCε. Adapted from [32].

However, unconjugated or native PKCε+ requires the use of cell permeabilization methods (i.e., saponin treatment) for efficacious intracellular targeting to exert cardioprotective effects [34]. This provides challenges in *ex vivo* and *in vivo* models where the integrity of the organs must be maintained for analysis. Therefore, conjugating PKCε+ to known intracellular delivery moieties may be a method to effectively activate PKCε for cardioprotection. Two empirically successful modifications of PKCε+ native peptide are myristic acid- (Myr) and transactivating peptide- (TAT) conjugated PKCε+ [6, 7].

TAT was originally an HIV-derived 86 amino acid peptide capable of penetrating the cell membrane [35]. It has since been discovered that residues 49-57 of TAT (RKKRRQRRR) are necessary and sufficient for internalization and serve as an efficient transduction domain [36]. The positively charged amino acid peptide presumably targets negatively charged proteoglycans on the plasma membrane and enters the cell through endocytosis [37] (Figure 3). While the complete mechanism by which TAT enters the cell has yet to be elucidated, there is evidence that the basic arginine-rich peptide uses three endocytic pathways simultaneously: macropinocytosis, clathrin-mediated endocytosis, and caveolar endocytosis [37]. Moreover, the unique shape and bonding capabilities of the positively charged guanidinuim group on arginine is essential in these endocytic processes [38]. Our study employs a undecapeptide conjugation (YGRKKRRQRRR) from residues 47-57 of TAT with a reducible C terminus disulfide bond (CC) to facilitate cargo release upon cellular internalization [39, 40]. Further, the hydrophilic nature of this moiety provides great potential for therapeutic applications. [24, 25].

The TAT transduction domain has been widely used as a method to enhance cellular uptake of PKCε+ in MI/R experiments to mimic IPC. In cardiac myocytes, TAT-conjugated

PKCε+ showed selective PKCε activation and translocation resulting in reduced adult cardiac myocyte damage and increased cell viability after prolonged hypoxia [32]. In *ex vivo* models, TAT-PKCε+ pretretament has been shown to decrease CK release, improve left ventricular developed pressure (LVDP), and reduce infarct size in Langendorff perfused rat hearts [7, 41]. The above studies used TAT-conjugated scrambled PKCε+, native PKCε+, and TAT alone as controls, all of which had no cardioprotective effects [7, 32, 41]. In regards to *in vivo* experiments, TAT-PKCε+ administered via intraperitoneal (IP) injection showed PKCε translocation in the heart, brain, liver, lung, and kidney in mice. Further, no signs of systemic toxicity were observed when TAT-PKCε+ was administered once a day for 14 days [42]. Collectively, these results suggest that TAT is an effective cellular delivery moiety for PKCε+.

By contrast, Myr is a lipophilic saturated fatty acid chain that enters the cell through simple diffusion [43] (Figure 3). The attached cargo then enters the cell through simple diffusion and is either released by an unknown cleavage mechanism or remains tethered to the fatty acid. It is also possible that transbilayer exchange allows the myristoylated peptide to enter the cell where it is targeted to other cellular membranes [44]. Although myristic acid-conjugated peptides are less soluble than TAT-conjugated peptides in physiologic buffers, they provide an efficacious mode of entry into various cell types due to their ability to enter the lipid bilayer independently of any supplemental moieties [44, 45]. Additionally, Myr conjugated peptides show rapid membrane association and homogenous distribution within cells which may provide an advantage over the slower process of endocytosis and endosomal release [44].

The effective cellular uptake of myristoylated peptides has also been demonstrated in several MI/R studies. In Langendorff perfused hearts, Myr-PKCε+ pretreatment showed

improved postreperfused LVDP and reduced polymorphonuclear leukocyte (PMN) infiltration after MI(20min)/R(45min +PMNs) [6]. By contrast, when given at reperfusion, myristoylated PKC peptide inhibitor (Myr-PKCε-) showed reduction in infarct size and concentration dependent improvement in postreperfused LVDP [46]. Additionally, an Myr-conjugated mitochondrial fission inhibitor (Myr-P110) was effective in restoring of postreperfused cardiac function and reducing infarct size in MI(30min)/R(90min) [47]. In toto, these results suggest that Myr-conjugation facilitates the intracellular targeting of small peptides.

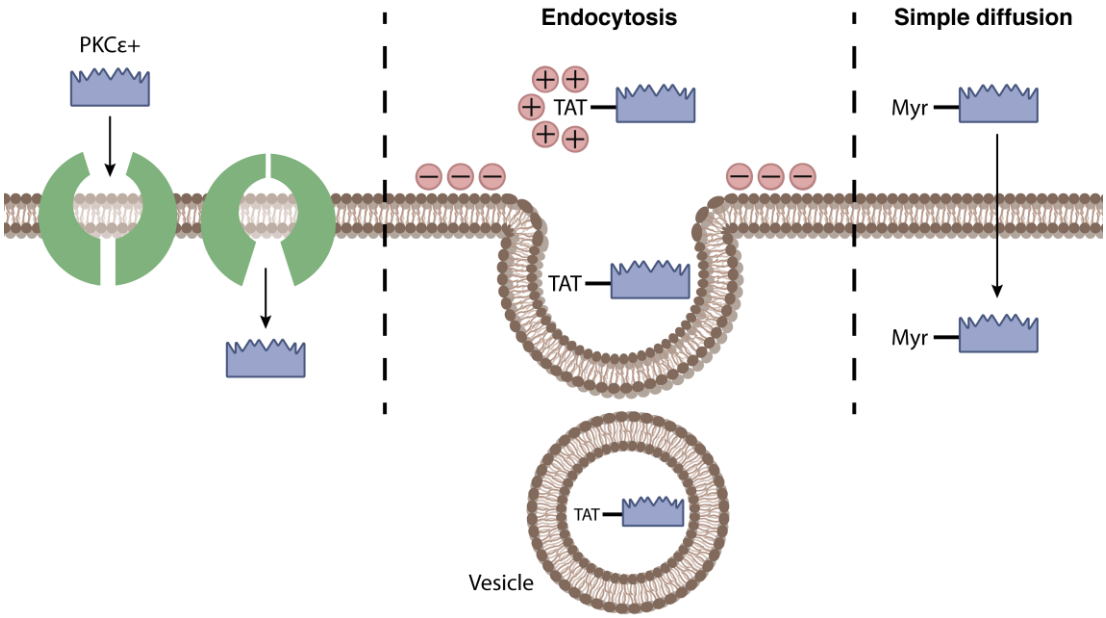

Figure 3. Mode of entry for PKCε+

Native peptide (left), TAT-conjugated peptide (middle), and Myr-conjugated peptide (right). Native PKCε+ presumably enters via facilitated diffusion, TAT-conjugated PKCε+ enters via endocytosis, and Myr- PKCε+ enters via simple diffusion.

While both moieties have been empirically proven to be effective in delivering cargo sequences to interact with intracellular targets, there are a limited number of studies directly comparing the effectiveness of cargo sequence delivery through these differing mechanisms in *ex vivo* MI/R.

1.2 Goal

Our study aims to use one MI(30min)/R(90min) model to directly compare the effects of native PKCε+, Myr-PKCε+, and TAT-PKCε+ pretreatment on cardiac contractile function and infarct size. Further, we wanted to assess whether any differences between these moieties exist in regards to infarct size reduction and restoration of postreperfused cardiac function.

1.2.1 Evaluating an extended reperfusion period for Myr-PKCε+

Additionally, this study will evaluate whether cell permeable PKCε+ would improve postreperfused cardiac function within a longer reperfusion time period (i.e. 90 min) than a previous study from our lab that used Myr-PKCε+ in MI(30 min)/R(45 min) [48].

1.2.2 Examining inter-method reliability between pixel and weight based infarct measurement

Previous studies in our lab have isolated and weighed infarcted versus viable tissue to determine infarct size (percent weight). While this method has been proven to be reliable, we wanted to explore a method in which we could minimize researcher bias and create an image archive that would allow for retrospective analysis. In this study, we began using NIH software ImageJ to trace pixels of infarcted area versus viable tissue to determine infarct size (percent pixels). We wanted to compare the reliability of using ImageJ pixel analysis to the previously used weight dissection analysis [46, 48].

1.3 Hypothesis

We hypothesize that pretreatment with Myr-PKCε+ and TAT-PKCε+ will attenuate infarct size using either percent weight or ImageJ pixel analysis, compared to native PKCε+ pretreated and untreated control hearts in MI(30 min)/R(90 min). This comparison has great therapeutic

value, as efficient intracellular drug delivery is central to improved histological and functional outcomes in heart attack/coronary bypass patients and organ transplant recipients.

In regards to infarct size measurement technique, we predict that ImageJ pixel analysis will yield potential for multiple and retrospective analyses to evaluate reproducibility of infarct size measurement. However, we expect that weight- and pixel-based analyses will show similar inter-method reliability.

METHODS

2.1 Heart isolation & Langendorff heart preparation to examine contractile function

Male Sprague-Dawley rats (275-325g, Charles River, Springfield MA) were anesthetized intraperitoneally with sodium pentobarbital (60 mg/kg) and anticoagulated with 1000 units heparin. The heart was then isolated from the rat and perfused through the ascending aorta with oxygenated Krebs' buffer (25mM NaHCO3, 17 mM dextrose, 5.9 mM KCl, 120 mM NaCl, 0.5 mM EDTA, 2.5 mM $CaCl_2$, and 1.2 mM $MgCl_2$) maintained at 36.5°C as previously described [46]. The aorta was secured onto the perfusion needle using surgical suture and was lowered into a reservoir filled with warmed Krebs' buffer. A constant pressure of 80mmHg, pH of 7.35-7.45, and a temperature of 36.5°C was maintained throughout the experiment. Following a stable 15 minute equilibration period, hearts were pretreated with 5mL of buffer plus vehicle (0.028% DMSO) for the control hearts or 5 mL of drug pretreatment (PKCε+, Myr-PKCε+, TAT-PKCε+; 10μM) dissolved in buffer at 1 mL/min infusion rate for 5 min immediately prior to 30 minutes of global ischemia. After 30 minutes of ischemia, the buffer flow was resumed for a 90-minute reperfusion period. A recording was taken every 5 min throughout the experiment (baseline, pretreatment infusion, ischemia, reperfusion) (Fig 3). Left ventricular end systolic pressure (LVESP), left ventricular end diastolic pressure (LVEDP), heart rate, coronary flow, and maximum (+dP/dtmax) and minimum (-dP/dtmin) rate of pressure change in the left ventricle were measured using a microtip pressure catheter (SPR-524; Millar Instruments, Inc., Houston, TX) inserted into

the left ventricle every 5 minutes throughout the equilibration, infusion, and reperfusion period. LVDP was calculated as the difference between LVESP and LVEDP.

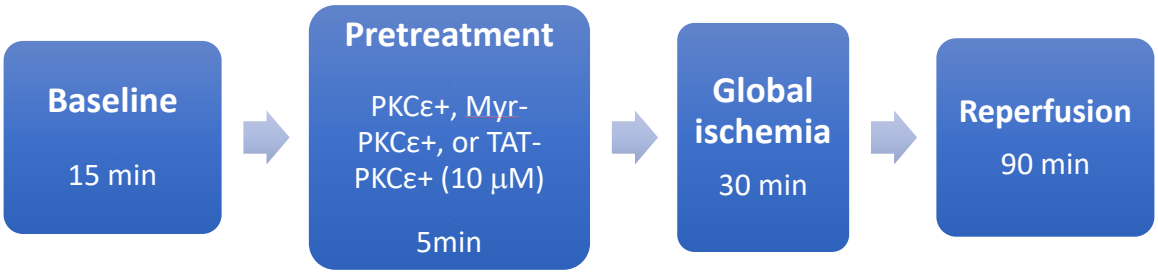

Figure 4. Experimental protocol in the Langendorff perfused heart.
MI(30min)/R(90min)followed a 15 min equilibration period and 5 min infusion period.

2.1.1 Peptide formulations

Activator peptides Myr-PKCε+, TAT-PKCε+, and native PKCε+ were purchased from Genemed Synthesis Inc., *San Antonio TX*. Native PKCε+ (HDAPIGYD) octapeptide is a linear amino acid sequence. Myr is a saturated fatty acid, also known as 1-tetradecanoic acid ($CH_3(CH_2)_{12}COOH$), which was conjugated to the octapeptide PKCε+. TAT (YGRKKRRQRRR) is conjugated to PKCε+ via a cysteine-cysteine double bond to facilitate free cargo delivery (Table 1).

Table 1. PKCε activator peptide purity, sequence, and molecular weight.

Peptide	**Purity (%)**	**Sequence**	**Molecular weight (g/mol)**
Myr-PKCε+	>95%	$CH_3(CH_2)_{12}COOH$-HDAPIGYD	1097
TAT-PKCε+	>95%	YGRKKRRQRRR-CC-HDAPIGYD	2632
Native PKCε+	>95%	HDAPIGYD	887

2.1.2 Determination of drug concentration

10μM final infusion concentration was chosen based on its ability to maximally stimulate coupled eNOS activity as pretreatment therefore increasing NO release [6, 29]. Further, the 10μM concentration was used in previous studies in our lab assessing pretreatment with Myr-PKCε+ in an MI(30min)/R(45min) model [48].

2.1.3 Drug dose/preparation

100 μL drug stock solutions were prepared for pretreatment infusion. Myr-PKCε+, TAT-PKCε+, and native PKCε+ (HDAPIGYD, MW= 887 g/mol) were solubilized separately in 28% DMSO, 1% 1N HCl, and 71% diH_2O. This drug preparation was based on the empirically-determined minimum solubility requirements of the myristic acid-conjugated peptide (Myr-PKCε+). Drug stock was further solubilized in 5mL of Kreb's buffer for infusion and adjusted for coronary flow for a final 10 μM drug concentration upon infusion prior to global ischemia. Final vehicle concentration was 0.028% DMSO and 0.001% HCl.

2.1.4 MI/R hearts: Untreated control

Following a 15 minute equilibration period, 5mL of buffer containing 28 μL DMSO, 1 μL 1N HCl, and 71 μL diH_2O was infused into the heart, followed by 30 minutes of global ischemia. The untreated MI/R control group allows one to analyze cardiac function and infarct size data for hearts that are treated with and without PKCε+ peptides and confirms negligible effect of vehicle on the heart.

2.1.5 MI/R hearts: drug treated (PKCε+, Myr-PKCε+, TAT- PKCε+)

Drug treated hearts were subjected to the same I/R periods and conditions as untreated control hearts with the exception of the 5 mL buffer pretreatment containing PKCε+, Myr-PKCε+, or TAT- PKCε+ at a final concentration of 10 μM in the perfusate.

2.1.6 Animal Care

Lab animals were from Charles River Laboratories Inc., Springfield MA. They were 12:12-h light:dark cycle and given 24 hour access to food and water. Male Sprague Dawley rats were fed normal chow ad libitum and used for experiments at 275-325g. All experiments were performed in accordance with the PCOM IACUC protocols A15-001 and A18-004.

2.2 Histological TTC staining to measure infarct size

After the 90 min reperfusion period, hearts were removed from the perfusion needle, and frozen at -20°C for 30 minutes. The hearts were then dissected into 2 mm pieces in rat heart slicer matrix with 2 mm transverse section slice intervals from apex to base and stained with 1% Triphenyltetrazolium chloride (TTC) in Tris buffer (pH = 7.41) at 37°C for 5 minutes. Viable tissue was stained red and necrotic tissue remained unstained. Afterward, the tissue was fixed in 4% paraformaldehyde overnight to enhance contrast of the stain.

2.2.1 ImageJ pixel analysis

For image analysis assessment, the infarcted area was calculated using NIH ImageJ software. Heart sections were partially flattened between plexiglass slides with 2mm spacers and photographed on both sides (superior and inferior). Infarcted area was traced

to measure pixels on both the superior and inferior portions of each heart section and averaged to get the infarcted pixel area of each section. Infarcted area was normalized to the total pixel area of each heart. Multiple analyses of infarcted pixel area were conducted for each experiment and calculated values were averaged.

2.2.2 Weight dissection analysis

For weight analysis assessment, sections viable and dead tissue were weighed (total). The necrotic tissue was weighed and divided by the total weight to determine the infarct size as previously described [22].

2.3 Statistical Analysis

All data in the figures are presented as means ± S.E.M. ANOVA analysis using Student-Neuman-Keuls test was used to assess statistical difference in infarct size and cardiac function between untreated control I/R and PKCε+ I/R hearts. The same statistical analysis was used to evaluate measurements of individual assessments by ImageJ pixel analysis and weight analysis of TTC stained hearts. Probability values of < 0.05 were considered statistically significant.

RESULTS

3.1 Examination of infarct size in response to PKCε+ pretreatment

When assessed using NIH ImageJ software to determine percent of infarcted pixel area compared to total pixel area of the heart after TTC staining, hearts pretreated with Myr-PKCε+ or TAT-PKCε+ showed significant reduction in infarct size to 29±1% ($p<0.05$, n=6) or 25±2% ($p<0.01$, n=6) respectively compared to untreated control (35±2%, n=6) or native PKCε+ pretreated I/R hearts (34±2%, n=6). By contrast, native PKCε+ pretreated I/R hearts did not show significant reduction in infarct size and exhibited similar infarct size to that of untreated controls (Figure 5). This analysis was done in a single-blind manner in which the treatment group was withheld from research assistants analyzing the stained images of heart sections. Further, multiple researchers were assigned to each experiment and their infarct analyses were averaged to determine a mean infarct size for each experiment.

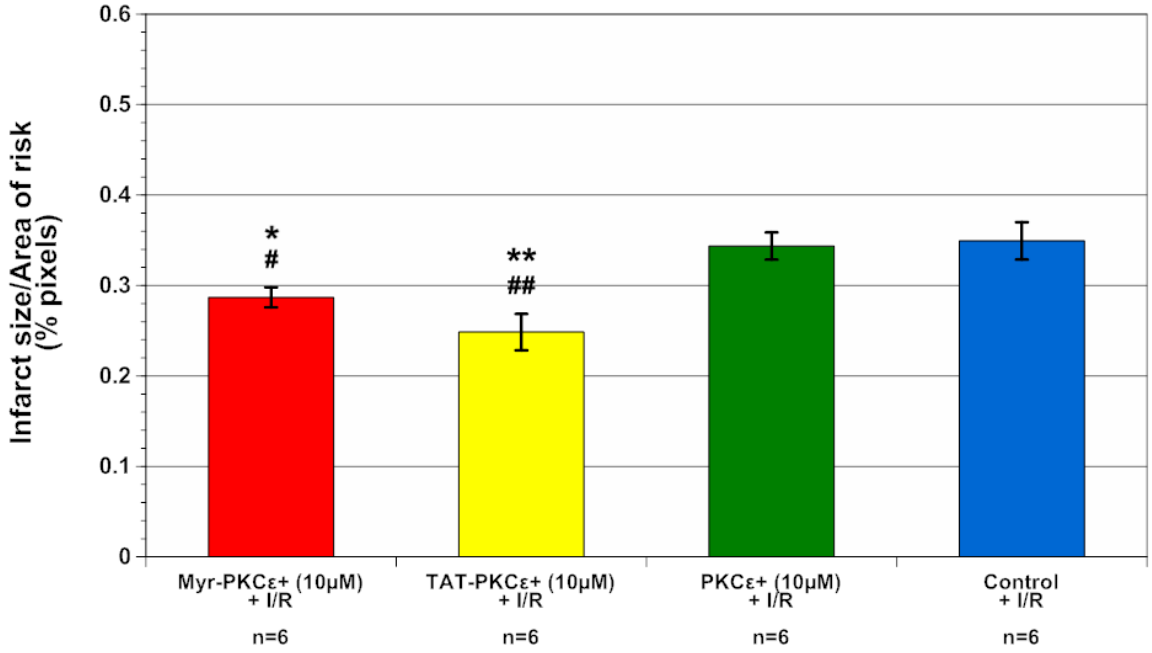

Figure 5. Percent pixel area infarct size.

*Percent infarct size of Myr-PKCε+ (10 μM) I/R (red), TAT-PKCε+ (10 μM) I/R (yellow), native PKCε+ (10 μM) I/R (green), and untreated control I/R (blue) expressed as percent pixels of total heart pixel size using NIH ImageJ software after TTC staining. Myr-PKCε+ and TAT-PKCε+ pretreatment significantly reduced infarct size to 29±1% and 25±2% respectively compared to untreated control hearts, 35±2%. Myr-PKCε+ and TAT-PKCε+ pretreated hearts also showed significant reduction in infarct size compared to native PKCε+. Native PKCε+ pretreated hearts showed similar infarct size to untreated controls and was not significantly different, 34±2%. *p < 0.05 vs. untreated control I/R, ** p < 0.01 vs. untreated control I/R, #p < 0.05 vs. native PKCε+, ##p < 0.01 vs. native PKCε+*

When assessed by dissection to determine percent infarcted weight of total heart weight after TTC staining, only TAT-PKCε+ pretreatment significantly reduced infarct size to 26±2% ($p<0.01$, n=6) compared to native PKCε+ pretreatment and untreated control I/R hearts which showed infarct size of 35±2% (n=6) and 36±2% (n=6) respectively. Myr-PKCε+ pretreatment reduced infarct size to 30±2% (n=6), but this was not significantly different from untreated controls. Native PKCε+ pretreated hearts showed similar infarct size to untreated control I/R hearts, 35±2% (n=6) and 36±2%

(n=6) respectively (Figure 6). This analysis was not blinded and percent infarcted weight was determined by only one researcher who performed the dissection 24 hours after each experiment after heart sections had been photographed.

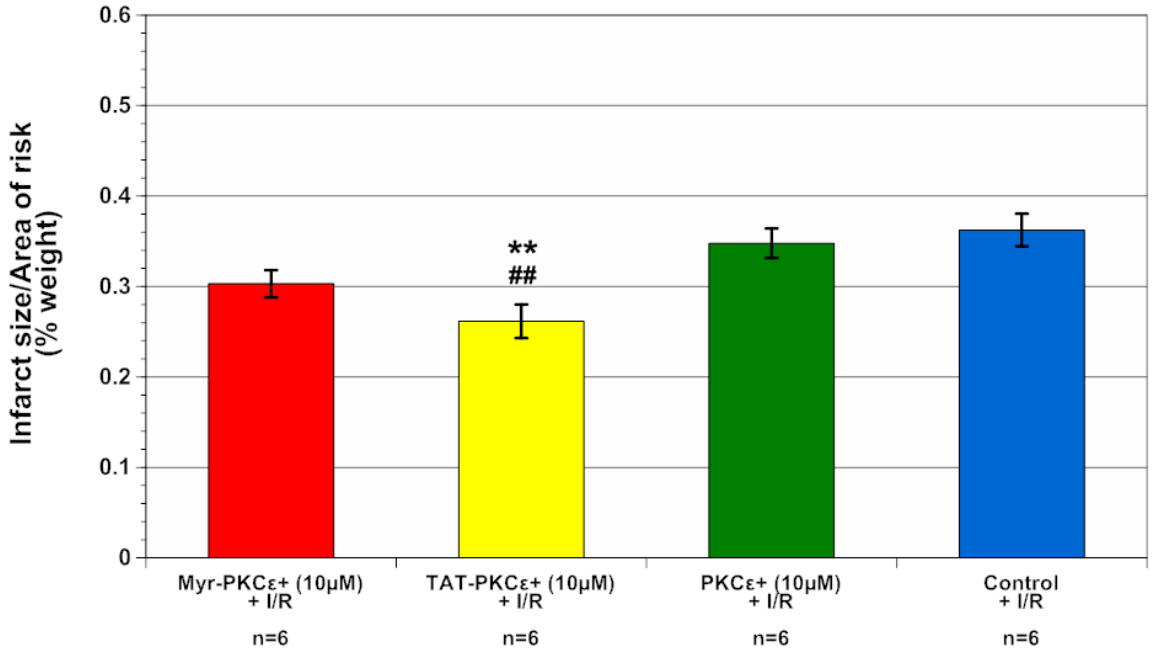

Figure 6. Percent weight infarct size.

*Percent infarct size of Myr-PKCε+ (10 μM) + I/R (red), TAT-PKCε+ (10 μM) + I/R (yellow), native PKCε+ (10 μM) + I/R (green), and untreated control I/R (blue) expressed as percent of total heart weight after TTC staining. TAT-PKCε+ pretreatment significantly reduced infarct size to 26±2% compared to untreated control and native PKCε+ hearts which exhibited a 36±2% and 35±2% reduction in infarct size respectively. Myr-PKCε+ and native PKCε+ pretreatment did significantly reduce in infarct size, 30±2% and 35±2% respectively, compared to untreated controls. ** p < 0.01 vs. untreated control I/R, ##p < 0.01 vs. native PKCε+*

3.2 Comparison of % pixel vs. % weight methods based on either total pixels or total weight

To assess inter-method reliability between the pixel and weight based methods we performed an ANOVA analysis using Student-Neuman-Keuls test. TAT-PKCε+

pretreated exhibited 25±2% (n=6; % pixels) and 26±1% (n=6; % weight) reduction in infarct size and was significantly different from both untreated control and native PKCε+ pretreated I/R hearts in both analyses ($p<0.01$). Similarly, Myr-PKCε+ pretreatment reduced infarct size to 29±1% (n=6; % pixels) and 30±2% (n=6; % weight) but was only determined to be significantly different from untreated control and native PKCε+ pretreated I/R hearts in the ImageJ analysis of pixel area method ($p<0.05$). By contrast, native PKCε+ pretreated showed 34±2% (n=6; % pixels) and 35±2% (n=6; % weight) infarct which was not significantly different from untreated controls, 35±2% (n=6; % pixels) and 36±2% (n=6; % weight), using either method of infarct size analysis. In general, the ImageJ analysis yielded slightly lower infarct size for all groups when compared to the dissection analysis. Although these two methods presented slightly different significance in results, they were not significantly different from each other (Figure 7).

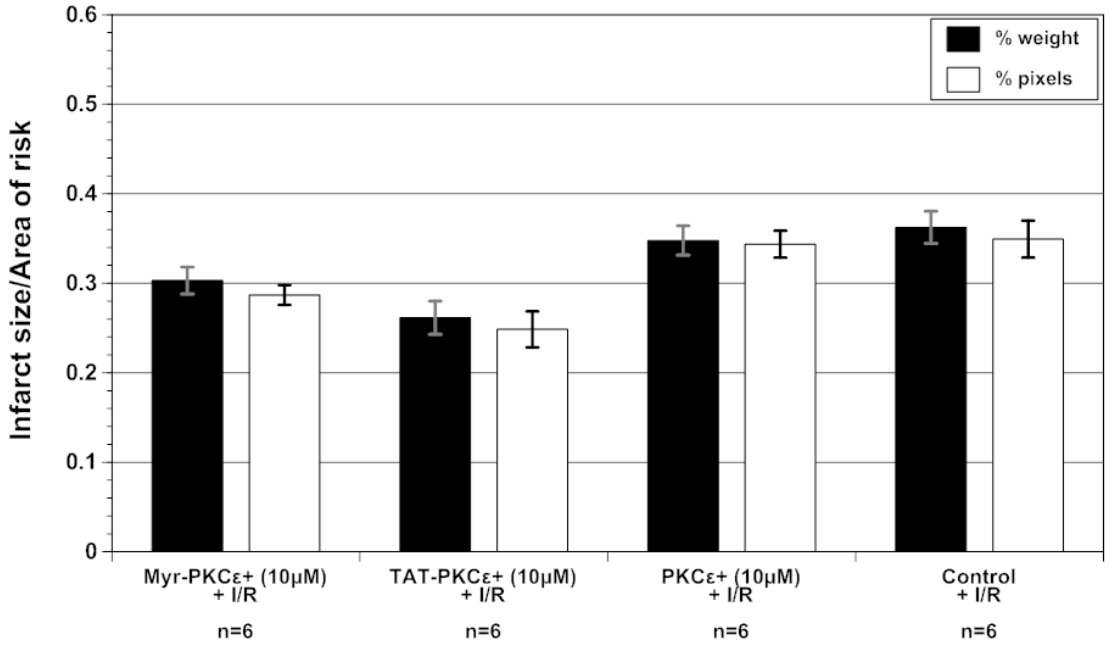

Figure 7. Comparison of infarct size analysis using dissection to determine percent infarct of total weight and ImageJ to determine percent pixels of total pixel area.

Infarct size is shown as both percent weight (black) as determined by dissection and percent pixels (white) measured using ImageJ. Myr-PKCε+ (10 μM) I/R, TAT-PKCε+ (10 μM) I/R, native PKCε+ (10 μM) I/R, and untreated control I/R showed no significant difference within groups using either method.

3.3 Examination of cardiac performance in response to PKCε+ pretreatment

Despite differences in infarct size, there was no significant difference in $+dP/dt_{max}$, $-dP/dt_{min}$, or LVDP across all groups tested (Table 2). Myr-PKCε+, TAT-PKCε+, native PKCε+, and untreated control hearts restored post-reperfused LVDP to 35±7%, 40±9%, 32±5%, and 38±5% of baseline values respectively (Figure 8). Interestingly, Myr-PKCε+ pretreatment exhibited significant improvement in post-reperfused LVEDP to 49±10 mmHg ($p<0.05$, n=6) compared to TAT-PKCε+, native PKCε+, and untreated control I/R hearts which restored LVEDP to 65±6 (n=6), 71±4 (n=6), and 71±4 mmHg (n=6) respectively. Myr-PKCε+ pretreatment also exhibited significant reduction of LVESP to 79±8 mmHg ($p<0.05$, n=6) compared to TAT-PKCε+, native PKCε+, and untreated control hearts which restored LVESP to 99±4 (n=6), 101±2 (n=6), and 105±4 mmHg (n=6) respectively (Table 2). These differences in LVEDP and LVESP did not result in a significant difference in LVDP (i.e., LVESP – LVEDP) because while LVEDP was significantly lowered, LVESP was significantly raised compared to other groups.

Table 2. Cardiac function values for all groups.

*Cardiac function initial (baseline) and final values for Myr-PKCε+ (10 μM) I/R (red), TAT-PKCε+ (10 μM) I/R (yellow), native PKCε+ (10 μM) I/R (green), and untreated control I/R (blue) hearts. Myr-PKCε+ pretreatment exhibited significant improvement in post-reperfused LVEDP to 49±10 mmHg compared to TAT-PKCε+, native PKCε+, and untreated control I/R hearts which restored LVESP to 65±6, 71±4, and 71±4 mmHg respectively. Myr-PKCε+ pretreatment also exhibited significant reduction of LVESP to 79±8 mmHg compared to TAT-PKCε+, native PKCε+, and untreated control I/R hearts which restored LVESP to 99±4, 101±2, and 105±4 mmHg respectively. *p < 0.05 vs. untreated control I/R, TAT-PKCε+ I/R and PKCε+ I/R*

	Myr-PKCε+ (10μM) I/R (n=6)	**TAT-PKCε+ (10μM) I/R (n=6)**	**PKCε+ (10μM) I/R (n=6)**	**Control I/R (n=6)**
Initial LVESP (mmHg)	95.4 ± 2.8	92.7 ± 2.4	101.5 ± 5.4	97.9 ± 2.5
Initial LVEDP (mmHg)	8.6 ± 0.8	8.4 ± 1.6	9.6 ± 2.9	9.9 ± 1.6
Initial LVDP (mmHg)	86.9 ± 2.6	84.3 ± 1.8	92.0 ± 3.5	88.0 ± 3.0
Final LVESP (mmHg)	*79.4 ± 7.6	98.8 ± 3.9	100.4 ± 2.0	104.7 ± 3.6
Final LVEDP (mmHg)	*48.8 ± 9.8	64.9 ± 6.4	70.7 ± 4.3	71.3 ± 4.3
Final LVDP (mmHg)	30.6 ± 5.8	33.9 ± 8.1	29.7 ± 4.9	33.4 ± 4.6
Initial +dP/dt$_{max}$ (mmHg/s)	2335.1 ± 101.3	2083.3 ± 46.0	2176.1 ± 90.9	2287.5 ± 61.8
Final dP/dt$_{max}$ (mmHg/s)	607.6 ± 135.9	694.8 ± 204.9	591.5 ± 85.0	743.2 ± 98.6
Initial dP/dt$_{min}$ (mmHg/s)	-1620.9 ± 88.0	-1375.7 ± 42.6	-1527.1 ± 67.2	-1557.7 ± 34.9
Final -dP/dt$_{min}$ (mmHg/s)	-403.4 ± 80.6	-517.6 ± 96.7	-501.8 ± 58.5	-484.1 ± 62.4
Initial Coronary Flow (mL/min)	21.8 ± 1.3	20.5 ± 1.9	22.6 ± 2.0	21.0 ± 1.2
Final Coronary Flow (mL/min)	6.3 ± 0.6	6.6 ± 0.9	7.4 ± 1.1	6.5 ± 0.9
Initial Heart Rate (BPM)	311.1 ± 16.2	284.0 ± 9.5	282.3 ± 10.2	294.0 ± 10.1
Final Heart Rate (BPM)	227.0 ± 20.9	245.8 ± 15.5	249.8 ± 15.5	249.1 ± 9.6

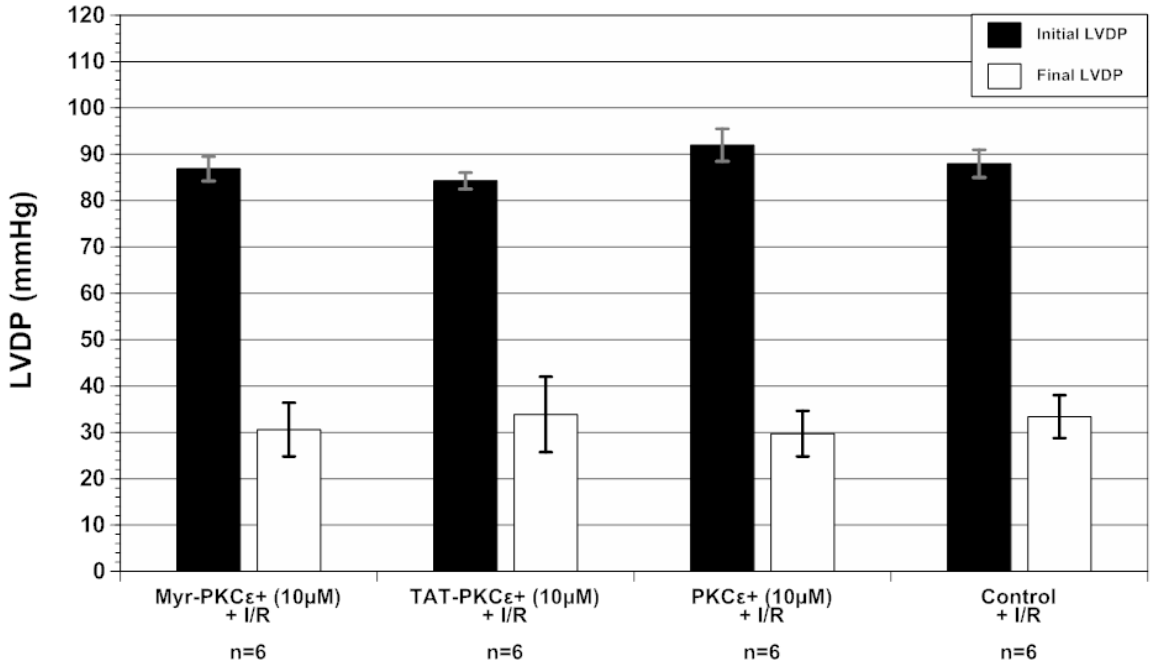

Figure 8. Initial and final LVDP values showed no difference across all groups.

Initial (black) and final (white) LVDP expressed in mmHg from isolated perfused rat hearts during stable baseline recordings before pretreatment and ischemia (initial) and after 90 min reperfusion (final). Myr-PKCε+, TAT-PKCε+, and native PKCε+ pretreatment I/R hearts recovered to 35±7%, 40±9%, and 32±5% of baseline values respectively. No group exhibited a significant improvement in final LVDP compared to untreated controls which recovered to 38±5% of baseline values.

DISCUSSION

4.1 Summary of results

4.1.1 TAT-PKCε+ and Myr-PKCε+ attenuate infarct size

TAT-PKCε+ pretreatment showed significant reduction in infarct size compared to native PKCε+ pretreatment and untreated control I/R hearts in both pixel and weight analyses. Similarly, Myr-PKCε+ pretreatment I/R hearts showed a significant reduction in infarct size when assessed by pixels (29%) when compared to native PKCε+ pretreatment and untreated control I/R hearts. However, the reduction in infarct size conferred by Myr-PKCε+ pretreatment was not significant in the weight analysis (30%). These results indicate that PKCε activation is cardioprotective before prolonged ischemia. Moreover, native PKCε+ did not significantly reduce infarct size (pixels=34%, weight=35%) compared to untreated I/R controls by either mode of infarct analysis (see Figures 5 and 6). Our results confirm that PKCε+ (HDAPIGYD) requires a cell permeable moiety for effective intracellular delivery and activation of PKCε to attenuate necrosis after prolonged ischemia. Further, TAT-conjugated PKCε+ may be superior to Myr-PKCε+ in reducing infarct size and facilitating PKCε preconditioning effects in MI/R.

By contrast, Nelson et al. would suggest that Myr conjugation is more efficacious than TAT conjugation for cargo sequence delivery, particularly in non-TAT permeant lymphocyte derived cells. However, their study looked at a murine B lymphocyte cell line (BA/F3) versus isolated organ preparations [44]. By comparison Patel et al. also

showed that Myr-conjugated Nox2 peptide inhibitor (Myr-peg gp91ds) was more efficacious in reducing PMN superoxide release compared to TAT-gp91ds [49]. Regarding whole organ preparation, Benjamin et al. showed that Myr-P110, a mitochondrial fission inhibitor, was more effective than TAT-P110 in restoring postreperfused cardiac function and reducing infarct size [47]. It should be noted that Benjamin et al. looked at specifically inhibiting a component of mitochondrial fission which is more limited in its targets than the many targets (i.e., 36) of PKCε [13]. It is plausible to speculate that the Myr-P110 may have had better permeabilization and efficient targeting due to the smaller size of P110 and being localized to one specific target (Drp1/fis1 interaction) which is localized on the outer mitochondrial membrane versus Myr-PKCε+ which has many targets, which are not all localized to cellular membranes.

In regards to the translocation mechanism of TAT, it is possible that processes other than endocytosis contributed to rapid intracellular delivery. Interestingly, Ter-Avetisyan et al. showed TAT transduction into BHK21 (C-13) fibroblasts in clathrin-mediated and caveolin-mediated endocytosis knock-outs as well as in fibroblasts incubated at 4°C. These results suggest that TAT is taken up into the cell in a process independent of endocytosis, presumably through direct penetration of the plasma membrane [50]. There are other reports showing that highly cationic peptides (R_{6-8}) may enter the cell through spontaneous translocation through the plasma membrane. However, these studies require high peptide concentrations above a minimum threshold or conditions in which strong membrane binding occurs [37]. Taken together, the multiple

mechanisms by which TAT may enter the cell may have contributed to the efficient and effective uptake of TAT-PKCε+ in our experiments.

4.1.2 ImageJ pixel analysis versus dissection weight analysis of infarct size

Collectively, infarct size across all groups was slightly reduced when analyzed using ImageJ compared to the weight dissection analysis, but this difference was not significant. This may be attributed to the uneven distribution of infarcted area between the superior and inferior side of each transverse myocardial cross-section. ImageJ pixel area was calculated as the average of infarcted area on the superior and inferior portions of each section. Interestingly, the ImageJ pixel analysis of infarct size more accurately supports our working hypothesis that cell permeable conjugated PKCε+ (i.e. Myr-PKCε+ and TAT-PKCε+) exhibited a greater reduction in infarct size than native PKCε+ which was no different than untreated control hearts. By contrast, the weight dissection analysis of infarct size showed that only TAT-PKCε+ pretreatment significantly reduced infarct size when compared to native PKCε+ and untreated control I/R hearts. In this regard, the data from the weight based infarct analysis did not completely support our hypothesis. Regardless, the results from this study would suggest that both methods are a reliable way for which to measure infarct size after TTC staining since they did not differ from each other. This supports our original hypothesis that both methods of measuring infarct size show similar inter-method reliability (Figure 7).

One of the advantages of doing pixel reading is that images are archived and multiple analyses of the data are possible in a single-blind manner. This allows for a retrospective study analysis in which current data may be reanalyzed and compared to other agents in future studies. By contrast, weight infarct analysis sometimes, but not

always, entails a person who is familiar with the conditions of the experiment and is therefore prone to researcher bias. Moreover, this method can only be performed one time and, although it is designed that the same person will isolate the infarct versus viable tissue, that is not always the case. As scientists try to do their best to be accurate, the fact that we have limited people analyzing the weight method is limiting in itself and perhaps could have contributed to the lack of significant reduction in infarct size after Myr-PKCε+ pretreatment versus the total blinded pixel based method (i.e., ImageJ). In conclusion, the pixel method may be superior to the weight method because there is less bias, there are more opportunities (i.e. number of people) to analyze the infarct area, it allows for comparison across studies, and it is not time sensitive.

4.1.3 Cardiac Function

Despite reduction in infarct size, none of the PKCε+ treated groups showed significant recovery of cardiac function throughout the reperfusion period compared to untreated control hearts. Interestingly, Myr-PKCε+ pretreated exhibited significantly improved LVEDP compared to TAT-PKCε+, native PKCε+, and untreated control hearts, but this did not manifest in an improved LVDP due to significantly reduced LVESP (see Table 2 and Figure 8). These results indicate that the infarct sparing effect of pretreatment with PKCε is independent of function recovery. These results are also consistent with an earlier pilot study from our lab which showed that Myr-PKCε+ reduced infarct size to 23% but did not restore cardiac function compared to untreated controls using a similar ischemic time period (i.e. 30min) and a shorter reperfusion time period (i.e. 45min) [48]. Our study was aimed at resolving whether cardiac function could be restored at a longer reperfusion time modality. Our recently published work using

Myr-PKCε peptide inhibitor (Myr-PKCε-, 20 μM) showed a delayed improvement in cardiac function from 60 to 90 min [46]. This led us to explore the length of the reperfusion timecourse in this study to see if there could be an improvement in cardiac function that was not seen during the 45 min reperfusion period.

4.1.4 The dichotomy between infarct size and cardiac function

Interestingly, Saurin et al. reported no difference in LVDP in PKCε$^{-/-}$ knockout mice and mice with the full complement of PKCε protein (PKCε$^{+/-}$ heterozygous) in MI(45 min)/R(90 min). Although PKCε$^{-/-}$ mice were resistant to the cardioprotective effects of IPC (i.e. infarct size reduction), postreperfused LVDP was preserved and similar to that of IPC preconditioned PKCε$^{+/-}$ mice [4]. Although PKCε deficient mice recovered LVDP, these results support our conclusion that the infarct sparing effects of PKCε may be independent of contractile recovery.

Myocardial stunning provides another possible explanation for lack of contractile recovery despite reduction in infarct size. Kloner et. al showed that mitochondrial directed antioxidant (SS-31) given at reperfusion reduced infarct size in three different animal models. However, one of the animal models did not show restoration in cardiac function despite showing reduction in infarct size [51]. Their explanation for this is that the heart may have been stunned. Myocardial stunning is a phenomenon during which asynchrony in the stunned myocardium impedes the ability of the organ to recover. However, this contractile deficit is reversible as cardiomyocytes salvaged by reperfusion are still viable [52]. It is quite plausible in this ischemia model that stunning could persist throughout the timecourse in these experiments. It is also possible that diminished

coronary flow at reperfusion leads to hibernation. This type of postischemic dysfunction is defined as chronic depression of function and is thought to be an alternative protective mechanism in which the heart responds to reduced O_2 supply by downregulating cardiac function and metabolism [53].

Nevertheless, reduction in infarct size is of great clinical relevance. Scar tissue, measured by late gadolinium-enhanced (LGE) magnetic resonance imaging (MRI), has been shown to be a better predictor of future events than contractile reserve in patients with chronic MI [54]. In regards to acute MI, Wu et al. demonstrated that acute infarct size relates to LV remodeling and is a better predictor of long-term prognosis than cardiac function measurements (i.e. LV systolic performance) [55]. Therefore, infarct size reduction via cell permeable PKCε+ could improve the prognosis for patients who suffer from chronic and acute myocardial infarction.

4.1.5 Length of ischemic period and recovery of cardiac function

Another rationale for the disparity between infarct size and cardiac function in our experiments is the length of prolonged ischemia which plays a role in the extent to which the heart may recover at reperfusion. Inagaki et. al showed recovery of cardiac function when hearts were pretreated with TAT-PKCε+ during MI(20min)/R(40min), but did not report function data in their MI(40min)/R(120 min) model. It is plausible that the hearts did not recover after the 40 min ischemic period even though there was still a reduction in infarct size [7]. Teng et. al also used a MI(20min)/R(45min + PMNs) to simulate PMN mediated I/R dysfunction to mimic *in vivo* conditions where PMN infiltration is significant 3-4 hours post-reperfusion in regional MI/R injury [56, 57]. In this model,

hearts pretreated with Myr-PKCε+ (5μM) exhibited improved postreperfused LVDP and reduced PMN infiltration.

Taken together with our results in which cardiac function did not recover after 30 min of ischemia, it is plausible that 20 min of ischemia may not have been sufficient to irreversibly depress contractile function before the end of the reperfusion period. By contrast, going longer in ischemia (i.e., 30 min) cardiac function recovery was not observed with either cell permeable moiety despite reduction in infarct size. Extending the ischemic time period by 10 min may have caused prolonged myocardial stunning that cell permeable PKCε+ could not correct during the reperfusion time. Collectively, the lack of function recovery after a longer ischemic time periods (i.e., $\geq$ 30min) highlights the importance of clinical timing of intervention (i.e. angioplasty) in patients with acute myocardial infarction.

4.1.6 PKCε before prolonged ischemia and at the onset of reperfusion

Various studies have demonstrated that PKCε activation prior to prolonged ischemia, and not at reperfusion, is cardioprotective. Inagaki et. al demonstrated that TAT-PKCε+ (500 nmol/L) decreased CPK release and improved LVEDP, LVDP, and coronary vascular resistance (CVR) when administered prior to prolonged ischemia (i.e. 20 min) but not when administered at the onset of reperfusion in isolated perfused rat hearts [7]. Along the same lines, Teng et. al observed that Myr-PKCε+ (5 μM) pretreatment restored postreperfused LVDP to 90±10% of baseline values in isolated perfused rat hearts after 20 min ischemia with PMNs. This effect was not seen when Myr-PKCε+ was applied during reperfusion which restored LVDP to 75±7% of baseline

values and was not significantly different from untreated control hearts [6]. We therefore limited our study using PKCε+ only as pretreatment to determine which cell permeable moiety (i.e. TAT or Myr) provides more efficacious intracellular targeting.

Paradoxically, PKCε inhibition by PKCε- has been shown to be cardioprotective when administered at the onset of reperfusion [6, 29, 46, 48]. In the same study in which Myr-PKCε+ was used, Teng et. al demonstrated that Myr-PKCε- (5 μM) administered at the onset of reperfusion significantly attenuated cardiac contractile dysfunction and PMN adherence/infiltration after the 45 min reperfusion period [6]. In another study from our lab, Myr-PKCε- (5, 10, and 20 μM) given at reperfusion significantly reduced infarct size and Myr-PKCε- (10 and 20 μM) improved postreperfused LVDP during MI(30 min)/R(90 min) [46]. Although treatment at reperfusion may be more clinically relevant during acute myocardial infarction, pretreatment may be valuable when the timing of the ischemic event can be predicted such as during organ transplantation or coronary bypass.

4.2 Study Limitations

Although the Langendorff perfused heart provides a low cost, efficacious screening method to study a wide range of compounds to mitigate reperfusion injury, there are limitations. Organ isolation minimizes the number of confounding variables that can effect *in vivo* studies in which organ systems are integrated. However, *ex vivo* studies are less clinically relevant than *in vivo* studies. Although this preparation allows the study of the heart over the course of several hours which was sufficient for our MI(30 min)/R(90 min) experiments, it would be advantageous to monitor the heart for a longer period of time to determine if contractile function can be restored in the case of myocardial stunning. Moreover, Sutherland and Hearse report that there is a 5-10%

deterioration of contractile function per hour while being perfused in the Langendorff model [58]. Regardless of the above limitations, the Langendorff perfused heart preparation is highly reproducible, cost-effective, and well-suited to gain insightful data in pilot studies.

4.3 Future Studies

4.3.1 PKCε+ as pretreatment and PKCε- at reperfusion

It would be interesting to explore the opposite roles of PKCε in MI/R by pretreating hearts with cell permeable PKCε+ followed by PKCε- treatment at the onset of reperfusion. Small amounts of protective ROS are necessary to initiate an adaptive cardioprotective response before prolonged ischemia. PKCε activation as a preconditioning stimulus results in opening of mK_{ATP} channels and subsequent ROS release, which in turn activates a second pool of PKCε in the inner mitochondrial membrane to phosphorylate and close the MPTP [17]. However, these cardioprotective mechanisms are overwhelmed by increased ROS generation as a result of life-preserving reperfusion. Therefore, PKCε inhibition at reperfusion acts to inhibit uncoupled eNOS and further mK_{ATP} channel opening which attenuates ROS release [29, 60]. We predict PKCε activation as pretreatment and inhibition at reperfusion would have an additive effect and may result in improved cardiac function and even lesser infarct size in the Langendorff perfused heart.

4.3.2 Would promotion of eNOS coupling or eNOS uncoupling yield similar results to 20min ischemia model?

Perkins et. al demonstrated that promoting eNOS activity while simultaneously promoting eNOS coupling via Myr-PKCε+ and BH4 respectively at reperfusion resulted in increased NO release from rat femoral veins and improved postreperfused LVDP and +dP/dtmax in Langendorff perfused hearts. By contrast, when Myr-PKCε+ was applied at reperfusion to stimulate uncoupled eNOS activity in combination with BH2, there was increased H2O2 endothelial release and cardiac function did not recover [29]. While Perkins et. al evaluated the stimulation of coupled and uncoupled eNOS at reperfusion in MI(20min)/R(45min + PMNs), it would be interesting to use PKCε+ in combination with either BH_4 or BH_2 as pretreatment in MI(30 min)/R(90 min) to evaluate the role of coupled versus uncoupled eNOS activity. We are interested in evaluating whether promoting eNOS coupling before prolonged ischemia would still result in restoration of postreperfused cardiac function in this longer I/R protocol. The reason that this may be of value is that what we have recently learned from our research group that inhibiting uncoupled eNOS via Myr-PKCε- at reperfusion was still effective in MI(30 min)/R(90 min). However, the degree of restoration of postreperfused cardiac function was diminished from ~100% seen after 20 min ischemia by Perkins et. al to ~56% after 30 min ischemia [29, 46].

While NO release from coupled eNOS improves the coupling efficiency of the electron transport chain under normal conditions, it is possible that stimulation of uncoupled eNOS prior to prolonged ischemia results in small amounts of protective ROS [28]. Wang et. al found that sufficient concentrations of H_2O_2 pretreatment (i.e. 10-

100μM) are necessary to stimulate prosurvival pathways while low concentration H_2O_2 pretreatment (1μM) further aggravated I/R injury during MI(30min)/R(45min) [59]. Therefore, PKCε+ and BH_2 induced stimulation of uncoupled eNOS and subsequent superoxide release may propagate a protective signaling cascade which includes downstream PKCε activation in the inner mitochondrial membrane to open mitoK_{ATP} and prevent MPTP pore formation [17]. If this mechanism is helpful at longer ischemia times, this may be helpful for organ transplantation.

4.3.3 Visualizing native PKCε+, Myr-PKCε+, and TAT-PKCε+ within cardiomyocytes

In this study, efficacious intracellular targeting of PKCε+ and subsequent PKCε activation yielding cardioprotection was extrapolated by measuring physiological endpoints (i.e. contractile function and infarct size). Monitoring cargo translocation via a well-designed cellular assay would confirm successful intracellular delivery of these peptides and provide data on cellular distribution. Previous studies have used fluorescein peptide conjugations and fluorescence microscopy to visualize mechanism of entry and cellular distribution of cargo [44]. However, fluorescein would increase the size and hydrophobic characteristic of these molecules which could influence mode of entry into cells. Regardless, elucidating the mechanisms by which cell permeable peptides (i.e. Myr and TAT) enter the cell are of value due to their great therapeutic potential.

In regards to successful PKCε activation, a cellular assay measuring protein expression of phosphorylated eNOS in human umbilical vein endothelial cells (HUVECs) via western blot analysis could be used. HUVECs provide potential translation to human tissue, and eNOS is a known PKCε substrate which serves as principal ROS source in MI/R [6, 29]. This is described as being a key mechanism in mediating reperfusion

injury. Assessing differences in phosphorylated eNOS expression would be an effective method to determine how well PKCε+ is being delivered to cells and to assess potential differences between Myr- and TAT-conjugated PKCε+ delivery.

4.4 Significance of Findings

These results suggest that increasing cellular permeability of PKCε+ via conjugation to either Myr or TAT significantly improved its efficaciousness in attenuating infarct size when given prior to ischemia as a pharmacologic mimic of ischemic preconditioning. The results also suggest that Myr- or TAT-conjugated PKCε+ may be an effective treatment to attenuate cell death in coronary bypass, angioplasty, or organ transplantation settings.

REFERENCES

1. Roger VL. Epidemiology of myocardial infarction. *Med. Clin. North Am.* 2007; 91(4):537-52.
2. Hausenloy DJ, Yellon DM. Myocardial ischemia-reperfusion injury: A neglected therapeutic target. *J. Clin. Invest.* 2013; 123(1):92-100.
3. Murry CE, Jennings RB, Reimer KA. Preconditioning with ischemia: A delay of lethal cell injury in ischemic myocardium. *Circulation.* 1986; 74(5):1124-36.
4. Saurin AT, Pennington DJ, Raat NJ, Latchman DS, Owen MJ, Marber MS. Targeted disruption of the protein kinase C epsilon gene abolishes the infarct size reduction that follows ischaemic preconditioning of isolated buffer-perfused mouse hearts. *Cardiovasc. Res.* 2002; 55:672-80.
5. Budas GR, Churchill EN, Mochly-Rosen D. Cardioprotective mechanisms of PKC isozyme-selective activators and inhibitors in the treatment of ischemia-reperfusion injury. *Pharmacol. Res.* 2007; 55(6):523-36.
6. Teng JC, Kay H, Chen Q, Adams JS, Grilli C, Guglielmello G, Zambrano C, Krass S, Bell A, Young LH. Mechanisms related to the cardioprotective effects of protein kinase C epsilon (PKC epsilon) peptide activator or inhibitor in rat ischemia/reperfusion injury. *Naunyn Schmiedebergs Arch. Pharmacol.* 2008; 378(1):1-15.
7. Inagaki K, Hahn HS, Dorn GW 2nd, Mochly-Rosen D. Additive protection of the ischemic heart ex vivo by combined treatment with δ-protein kinase C inhibitor and ε-protein kinase C activator. *Circulation.* 2003;108(7):869-75.
8. Ping P, Song C, Zhang J, Guo Y, Cao X, Li RC, Wu W, Vondriska TM, Pass JM, Tang XL, Pierce WM, Bolli R. Formation of protein kinase cε-lck signaling modules confers cardioprotection. *J. Clin. Invest.* 2002; 109(4):499-507.
9. Ohnuma Y, Miura T, Miki T, Tanno M, Kuno A, Tsuchida A, Shimamoto K. Opening of mitochondrial K(ATP) channel occurs downstream of PKC-epsilon activation in the mechanism of preconditioning. *Am. J. Physiol. Heart Circ. Physiol.* 2002; 283(1):440-47.
10. Igumenova TI. Dynamics and Membrane Interactions of Protein Kinase C. *Biochemistry*. 2015; 54:4953−4968
11. Bogoyevitch, MA, Parker, PJ, Sugden, PH. Characterization of protein kinase C isotype expression in adult rat heart. Protein kinase C-epsilon is a major isotype present, and it is activated by phorbol esters, epinephrine, and endothelin. Circ. Res. 1993;72:757–767.
12. Disatnik MH, Buraggi G, Mochly-Rosen D. Localization of protein kinase C isozymes in cardiac myocytes. *Exp Cell Res*. 1994; 210(2):287-97.

13. Ping P1, Zhang J, Pierce WM Jr, Bolli R. Functional proteomic analysis of protein kinase C epsilon signaling complexes in the normal heart and during cardioprotection. *Circ Res*. 2001; 88(1):59-62.

14. Scruggs SB, Wang D, Ping P. *PRKCE* gene encoding protein kinase C-epsilon—Dual roles at sarcomeres and mitochondria in cardiomyocytes. *Gene*. 2016; 590:90–96.

15. Wang Y, Ashraf M. Role of protein kinase C in mitochondrial K(ATP) channel-mediated protection against Ca^{2+} overload injury in rat myocardium. *Circ. Res.* 1999; 84(10):1156-1164.

16. Budas GR, Churchill EN, Disatnik MH, Sun L, Mochly-Rosen D. Mitochondrial import of PKC1 is mediated by HSP90: a role in cardioprotection from ischaemia and reperfusion injury. *Cardiovasc Res*. 2010; 88:83–92.

17. Costa AD, Garlid KD. Intramitochondrial signaling: interactions among mitoKATP, PKCε, ROS, and MPT. *Am J Physiol Heart Circ Physiol*. 2008;295(2):H874-82.

18. Dorn GW 2nd, Force T. Protein kinase cascades in the regulation of cardiac hypertrophy. *J Clin Invest*. 2005; 115(3):527–537.

19. Brennan S, Jackson R, Patel M, Sims MW, Hudman D, Norman RI, Lodwick D, Rainbow RD. Early opening of sarcolemmal ATP-sensitive potassium channels is not a key step in PKC-mediated cardioprotection. *J Mol Cell Cardiol*. 2015; 79:42–53.

20. Sato T, O'Rourke B, Marbán E. Modulation of mitochondrial ATP-dependent K+ channels by protein kinase C. *Circ Res.* 1998; 83(1):110-4.

21. Gopalakrishna R, Jaken S. Protein kinase C signaling and oxidative stress. *Free Radic Biol Med.* 2000;28(9):1349-61.

22. Halestrap AP, Clarke SJ, Javadov SA. Mitochondrial permeability transition pore opening during myocardial reperfusion—a target for cardioprotection. *Cardiovasc Res.* 2004; 61(3):372-85.

23. Korge P, Honda HM, Weiss JN. Protection of cardiac mitochondria by diazoxide and protein kinase C: Implications for ischemic preconditioning. *Proc. Natl. Acad. Sci. U.S.A.* 2002; 99(5):3312-7.

24. Baines CP, Song CX, Zheng YT, Wang GW, Zhang J, Wang OL, Guo Y, Bolli R, Cardwell EM, Ping P. Protein kinase cε interacts with and inhibits the permeability transition pore in cardiac mitochondria. *Circ Res.* 2003; 92(8):873-80.

25. Mochly-Rosen D. Localization of protein kinases by anchoring proteins: A theme in signal transduction. *Science.* 1995; 268(5208):247-51.

26. Chen Q, Devine I, Walker S, Pham H, Ondrasik R, Patel H, Chau W, Parker CW, Bartol KD, Riahi S, Mittal A, Barsotti R, Young L. Nox2ds-Tat, A Peptide Inhibitor of NADPH Oxidase, Exerts Cardioprotective Effects by Attenuating

Reactive Oxygen Species During Ischemia/Reperfusion Injury. *Am J Biomed Sci*. 2016; 8(3):208-227.

27. Zhang J, Baines CP, Zong C, Cardwell EM, Wang G, Vondriska TM, Ping P. Functional proteomic analysis of a three-tier PKCε-Akt-eNOS signaling module in cardiac protection. *Am J Physiol Heart Circ Physiol*. 2005;288(2):H954-61.
28. Shen W, Tian R, Saupe KW, Spindler M, Ingwall JS. Endogenous nitric oxide enhances coupling between O2 consumption and ATP synthesis in guinea pig hearts. *Am J Physiol Heart Circ Physiol.* 2001; 281(2):H838-46.
29. Perkins KA, Pershad S, Chen Q, McGraw S, Adams JS, Zambrano C, Krass S, Emrich J, Bell B, Iyamu M, Prince C, Kay H, Teng JC, Young LH. The effects of modulating eNOS activity and coupling in ischemia/reperfusion (I/R). *Naunyn-Schmiedeberg's Arch Pharmacol*. 2012;385: 27–38.
30. Mochly-Rosen D, Khaner H, Lopez J. Identification of intracellular receptor proteins for activated protein kinase C. *Proc. Natl. Acad. Sci. U.S.A.* 1991; 88(9):3997-4000.
31. Mochly-Rosen D, Gordon AS. Anchoring proteins for protein kinase C: A means for isozyme selectivity. *FASEB J.* 1998; 12(1):35-42.
32. Dorn GW 2nd, Souroujon MC, Liron T, Chen CH, Gray MO, Zhou HZ, Csukai M, Wu G, Lorenz JN, Mochly-Rosen D. Sustained in vivo cardiac protection by a rationally designed peptide that causes epsilon protein kinase C translocation. *Proc. Natl. Acad. Sci. U.S.A.* 1999; 96(22):12798-803.
33. Chen L, Wright LR, Chen CH, Oliver SF, Wender PA, Mochly-Rosen D. Molecular transporters for peptides: Delivery of a cardioprotective εPKC agonist peptide into cells and intact ischemic heart using a transport system, R(7). *Chem. Biol.* 2001; 8(12):1123-9.
34. Johnson JA, Gray MO, Chen CH, Mochly-Rosen D. A Protein Kinase C Translocation Inhibitor as an Isozyme-selective Antagonist of Cardiac Function. *J Biol Chem*. 1996;271(40): 24962–24966.
35. Frankel AD, Pabo CO. Cellular uptake of the tat protein from human immunodeficiency virus. *Cell.* 1988;55(6): 1189-93.
36. Eguchi A, Akuta T, Okuyama H, Senda T, Yokoi H, Inokuchi H, Fujita S, Hayakawa T, Takeda K, Hasegawa M, Nakanishi M. Protein transduction domain of HIV-1 Tat protein promotes efficient delivery of DNA into mammalian cells. *J Biol Chem*. 276 (2001) 26204 – 26210.
37. Duchardt F, Fotin-Mleczek M, Schwarz H, Fischer R, Brock R. A Comprehensive Model for the Cellular Uptake of Cationic Cell-penetrating Peptides. *Traffic*. 2007;8: 848–866.
38. Mitchell DJ, Kim DT, Steinman L, Fathman CG, Rothbard JB. Polyarginine enters cells more efficiently than other polycationic homopolymers. *J Pept Res*. 2000; 56(5):318-25.

39. Saito G, Swanson JA, Lee KD. Drug delivery strategy utilizing conjugation via reversible disulfide linkages: role and site of cellular reducing activities. *Adv Drug Deliv Rev*. 2003; 55(2):199-215.

40. Lee SJ, Yoon SH, Doh KO. Enhancement of gene delivery using novel homodimeric tat peptide formed by disulfide bond. *J Microbiol Biotechnol*. 2011; 21(8):802-7.

41. Chen L, Hahn H, Wu G, Chen CH, Liron T, Schechtman D, Cavallaro G, Banci L, Guo Y, Bolli R, Dorn GW II, and Mochly-Rosen D. Opposing cardioprotective actions and parallel hypertrophic effects of δPKC and εPKC. *PNAS*. 2001; 98(20): 11114–11119.

42. Begley,R, Liron T, Baryza J, and Mochly-Rosen D. Biodistribution of intracellularly acting peptides conjugated reversibly to Tat. *Biochemical and Biophysical Research Communications 318* (2004) 949–954.

43. Young LH, Barsotti R, Benjamin I, Patel H, Dittakavi T, Chen Q. Comparing the Effects of Myristic Acid- and TAT- conjugated peptides to their native counterparts targeting intracellular pathways mediating myocardial ischemia/reperfusion injury and neutrophil superoxide release. *Curr Topics in Peptide and Protein Res.* 2016;17: 83-89.

44. Nelson AR, Borland L, Allbritton NL, Sims CE. Myristoyl-Based Transport of Peptides into Living Cells. *Biochemistry*. 2007;46(51):14771-14781.

45. McLaughlin S, Aderem A. The myristoyl-electrostatic switch: a modulator of reversible protein-membrane interactions. *Trends Biochem Sci*. 1995; 20(7):272-6.

46. McIntyre A, Adekayode C, Kim H, Woodley J, Dittakavi T, Finnegan M, Heron J, Amuquandoh K, James I, Benjamin I, Liu S, Walker K, Dean T, Hwang W, Chen Q, Barsotti R, Young LH. Protein Kinase C Epsilon Peptide Inhibitor Exerts Cardioprotective Effects in Myocardial Ischemia/Reperfusion Injury. *J Cardiobiol.* 2018; 5(1):6.

47. Benjamin I, Vu J, Lipscombe C, Stutzman D, Schmidgall C, Patel H, Patel S, Chen Q, Hatcher CJ, Barsotti R, Young LH. Comparison of the effects of myristoylated and transactivating peptide (TAT) conjugated mitochondrial fission peptide inhibitor (P110) in myocardial ischemia/reperfusion (I/R) injury. *Proceedings of the 24th American Peptide Symposium Michal Lebl (Editor) American Peptide Society.* 2015:143-46.

48. Montgomery M, Adams J, Teng J, Tekelehaymanot B, Ondrasik R, Devine I, Perkins KA, Chen Q, Barsotti R, Young LH. Myristoylated Protein Kinase C Epsilon Peptide Inhibitor Exerts Cardioprotective Effects in Rat and Porcine Myocardial Ischemia/Reperfusion: A Translational Research Study. *Proceedings of the 23rd American Peptide Symposium Michal Lebl (Editor) American Peptide Society*. 2013:178-79.

49. Patel H, Bartol K, Bottex A, Remarcke R, Chau W, Walker S, Chen Q, Barsotti R, Young LH. Comparing the effectiveness of TAT and Myristoylation of gp91ds

on leukocyte superoxide (SO) release. *Proceedings of the 24th American Peptide Symposium Michal Lebl (Editor) American Peptide Society*. 2015:150-53.

50. Ter-Avetisyan G, Tünnemann G, Nowak D, Nitschke M, Herrmann A, Drab M, Cardoso MC. Cell entry of arginine-rich peptides is independent of endocytosis. *J Biol Chem*. 2009;284(6): 3370-8.

51. Kloner RA, Hale SL, Dai W, Gorman RC, Shuto T, Koomalsingh KJ, Gorman JH 3rd, Sloan RC, Frasier CR, Watson CA, Bostian PA, Kypson AP, Brown DA. Reduction of ischemia/reperfusion injury with bendavia, a mitochondria-targeting cytoprotective peptide. *J Am Heart Assoc*. 2012;1(3):e001644.

52. Moens AL, Claeysa MJ, Timmermans JP, Vrints CJ. Myocardial ischemia/reperfusion-injury, a clinical view on a complex pathophysiological process. *Int J Cardiol*. 2005; 100(2):179-190.

53. Kim SJ, Peppas A, Hong SK, Yang G, Huang Y, Diaz G, Sadoshima J, Vatner DE, Vatner SF. Persistent stunning induces myocardial hibernation and protection: flow/function and metabolic mechanisms. *Circ Res*. 2003 Jun 13;92(11):1233-9. Epub 2003 May 15.

54. Kelle S, Roes SD, Klein C, Kokocinski T, de Roos A, Fleck E, Bax JJ, Nagel E. Prognostic value of myocardial infarct size and contractile reserve using magnetic resonance imaging. *J Am Coll Cardiol*. 2009;54(19):1770-7.

55. Wu KC, Zerhouni EA, Judd RM, Lugo-Olivieri CH, Barouch LA, Schulman SP, Blumenthal RS, Lima JA. Prognostic significance of microvascular obstruction by magnetic resonance imaging in patients with acute myocardial infarction. *Circulation*. 1998;97:765–72.

56. Tsao PS, Lefer AM. Time course and mechanism of endothelial dysfunction in isolated ischemic- and hypoxic-perfused rat hearts. *Am J Physiol*. 1990; 259:H1660–1666

57. Weyrich AS, Buerke M, Albertine KH, Lefer AM. Time course of coronary vascular endothelial adhesion molecule expression during reperfusion of the ischemic feline myocardium. *J Leukoc Biol*. 1995; 57:45–55

58. Sutherland FJ1, Hearse DJ. The isolated blood and perfusion fluid perfused heart. *Pharmacol Res*. 2000; 41(6):613-27.

59. Pomerantz BJ, Robinson TN, Heimbach JK, Calkins CM, Miller SA, et al. Selective mitochondrial KATP channel opening controls human myocardial preconditioning: Too much of a good thing? *Surgery*. 2000; 128:368-373.

60. Wang ZH, Liu JL, Wu L, Yu Z, Yang HT. Concentration-dependent wrestling between detrimental and protective effects of H_2O_2 during myocardial ischemia/reperfusion. *Cell Death and Disease.* 2014; 5:e1297